Lactate transporters in the rat barrel cortex sustains whisker-dependent BOLD fMRI signal and behavioral performance

Hélène Roumes[1,#], Charlotte Jollé[2,#], Jordy Blanc[1], Imad Benkhaled[1], Carolina Piletti Chatain[3], Philippe Massot[1], Gérard Raffard[1], Véronique Bouchaud[1], Marc Biran[1], Catherine Pythoud[4], Nicole Déglon[4], Eduardo Zimmer[5], Luc Pellerin[2,6,#] and Anne-Karine Bouzier-Sore[1,#,*].

[1] Univ. Bordeaux, CNRS, CRMSB, UMR 5536, F-33076 Bordeaux, France
[2] Department of Physiology, Univ. Lausanne, Lausanne, Switzerland
[3] Department of Biochemistry, Universidade Federal do Rio Grande do Sul, Porto Alegre, Brazil
[4] Laboratory of Cellular and Molecular Neurotherapies (LCMN), Neuroscience Research Center (CRN), Department of Clinical Neurosciences (DNC), Lausanne University Hospital, Univ. Lausanne, Lausanne, Switzerland
[5] Department of Pharmacology, Graduate Program in Biological Sciences: Biochemistry (PPGBioq) and Pharmacology and Therapeutics (PPGFT), Universidade Federal do Rio Grande do Sul, Porto Alegre, Brazil
[6] IRTOMIT, Inserm U1082, Univ. Poitiers et CHU Poitiers, F-86021 Poitiers, France
[#] Same contribution

* Anne-Karine Bouzier-Sore Univ. Bordeaux, CNRS, CRMSB, UMR 5536, F-33076 Bordeaux, France.
Tel : +33 (0) 47 30 44 24. Fax : +33 (0) 5 5 57 45 56. E-mail : akb@rmsb.u-bordeaux.fr
https://orcid.org/0000-0002-3470-0940

Classification
Biological Sciences, Neurosciences.

Keywords
Brain metabolism, Monocarboxylate transporter, fMRI, MRS, Learning, Memory.

Author Contributions
AKBS has conceived and designed the project, acquired and analyzed fMRI, *in vivo* and *ex vivo* MRS data and wrote the article. HR has acquired and analyzed MRI and NMR data, has performed rescue experiments and has contributed to the writing of this article. IB has performed BOLD fMRI quantifications. CJ has produced the MCT-KD animal, has set up and performed the behavioral studies and has contributed to the writing of this article. JB has acquired and analyzed MRI and NMR data, and has contributed to the rescue experiments. GR and PM have conceived the whisker activation MRI-compatible system. MB has acquired *ex vivo* MRS data. VB has prepared the perchloric acid extracts. ND and CP have designed and produced the AAV vectors. CC and EZ have contributed to the writing of this article. LP has contributed to the conception and design of the project, to data analyses and to the writing of this article.

Abstract

Lactate is an efficient neuronal energy source even in presence of glucose. However, the importance of lactate shuttling between astrocytes and neurons for brain activation and function remains to be established. For this purpose, metabolic and hemodynamic responses to sensory stimulation have been measured by fMRS and BOLD fMRI after downregulation of either neuronal MCT2 or astroglial MCT4 in the rat barrel cortex. Results show that the lactate rise in the barrel cortex upon whisker stimulation is abolished when either transporter is downregulated. Under the same paradigm, the BOLD response is prevented in all MCT2-downregulated rats while about half of the MCT4-downregulated rats exhibited a loss of the BOLD response. Interestingly, MCT4-downregulated animals showing no BOLD response were rescued by peripheral lactate infusion while this treatment had no effect on MCT2-downregulated rats. When animals were tested in a novel object recognition task, MCT2-downregulated animals were impaired in the textured but not in the visual version of the task. For MCT4-downregulated animals, while all animal succeeded in the visual task, half of the MCT4-downregulated rats exhibited a deficit in the textured task - a similar segregation into two groups as observed for BOLD experiments. Our data demonstrate that lactate shuttling between astrocytes and neurons is essential to give rise to both neurometabolic and neurovascular couplings, which form the basis for the detection of brain activation by functional brain imaging techniques. Moreover, our results establish that this metabolic cooperation is required to sustain behavioral performance based on cortical activation.

Significance Statement

For decades, it was claimed that glucose was the sole and sufficient energy substrate to sustain neuronal activity and brain function. Our results challenge this view by demonstrating that despite glucose availability, lactate shuttling from astrocytes to neurons *via* monocarboxylate transporters is necessary to give rise to the BOLD signal (used as a surrogate marker for activation) in the rat cerebral cortex following whisker stimulation. Moreover, lactate shuttling turned out to be also essential for sustaining behavioral performance associated with activation of the rat barrel cortex. These findings call for a reappraisal of neuroenergetics and the role of astrocytes in determining brain activation and function.

Introduction

In the past 25 years, a major revolution in the field of brain energy metabolism has occurred. While it was believed classically that glucose is the sole valuable energy substrate for neurons, it is now admitted that under certain circumstances, alternative substrates can serve as fuels and replace glucose, at least partially, even in the adult brain. This is the case for lactate. Indeed, it was shown that lactate provided from the periphery through the blood circulation is efficiently used by the brain in animals (1) and humans (2-4). In addition to peripheral supply, the brain itself has the capacity to internally produce lactate from peripheral glucose. This process of activity-dependent lactate transfer is named ANLS (5) and has received a large support in the literature based on *in vitro* (6, 7), *ex vivo* (1) and *in vivo* experiments (8-11). It was also shown that lactate supply by glial cells to neurons is a fundamental process that has been conserved during evolution as it was found to be present in invertebrates as well (e.g. flies) (12, 13). Nevertheless, some recent studies have provided evidence that direct glucose utilization by neurons also takes place during activation (14, 15). It might be essential for some aspects of neurotransmission (16) or when metabolized via the pentose phosphate pathway to regenerate glutathione and ensure antioxidant protection (17). These observations call for further *in vivo* investigations to assess the contribution of these energy supply modes to sustain brain activities ranging from metabolic and hemodynamic responses associated with brain activation to behavioral performances.

It has been well documented that activation of a brain region (e.g. hippocampus or cortex) leads to a transient increase in lactate concentration within the activated area in rodents (18-20) and in humans (21, 22). Such an observation might reflect a transient mismatch between lactate production attributed to astrocytes and utilization/disposal by other brain cells, although the importance of each remains to be confirmed *in vivo*. The capacity to release or utilize lactate is determined by the expression of specific transporters named monocarboxylate transporters (MCTs). Three members of this family have been identified in the central nervous system (23). MCT2 is the predominant neuronal lactate transporter (24). MCT4 expression is prominent on astrocytes (25) while MCT1 expression is more ubiquitous with strong expression on endothelial cells of blood vessels as well as on glial cells (26). Previously, it was shown that reducing MCT2 expression (which allows neuronal lactate uptake) interfered with blood oxygen level-dependent (BOLD) fMRI signal, which depends on local, activity-dependent change in blood flow and is used as a surrogate marker for neuronal activity to perform functional brain imaging (20).

1 Recently, new viral vector tools have been developed that allow the downregulation of either MCT2 or
2 MCT4 expression in a cell-specific manner *in vivo* (27). In the present study, we took advantage of this
3 approach to determine the importance of both transporters and by extension, of lactate shuttling
4 between astrocytes and neurons, in both metabolic and hemodynamic responses as well as in
5 behavioral performances associated with activation of the whisker-to-barrel system in rats.
6
7 **Results**
8 *Cortical lactate accumulation caused by whisker stimulation is prevented by either neuronal MCT2 or*
9 *astroglial MCT4 downregulation*
10
11 The impact of downregulating either the neuronal MCT2 or the astroglial MCT4 transporter in the rat
12 barrel cortex (S1BF area) on the metabolic response to whisker stimulation was evaluated by functional
13 MRS (fMRS) *in vivo*. Whiskers were stimulated directly into the magnet, using a MRI-compatible air-puff
14 system. The paradigm was composed of a succession of a 20 sec activation period (8 Hz) followed by
15 a 10 sec rest to avoid neuronal desensitization (**Figure 1A**)*. In vivo* ^{1}H-MRS was acquired in a 2x2.5x3
16 mm-voxel located in the left barrel cortex (**Figure 1B**). A first acquisition was performed at rest (**Figure**
17 **1B**, blue spectra). Then right whiskers were stimulated and a second acquisition was recorded (**Figure**
18 **1B**, red spectra). Functional MRS was performed in rats treated with a control adeno-associated vector
19 (AAV) expressing a non-specific sequence (Ctrl; white), or rats injected with vectors inducing the
20 knockdown MCT2 (MCT2-KD; purple) and MCT4-KD (orange). The signal from protons of the methyl
21 group of lactate is located at 1.32 ppm. The subtraction of the two spectra (activated – rest) is
22 represented in black. While an increase in lactate content in the barrel cortex can be observed in Ctrl
23 rats, this increase was abolished both in MCT2- and MCT4-KD rats. Quantification of metabolite
24 contents was performed using LCModel and the ratio [lactate content during whisker activation] over
25 [lactate content at rest] is presented in **Figure 1C**. This ratio was 1.25 ± 0.05 in control rats, a statistically
26 significant increase of 25% in lactate content during whisker activation, while this ratio was 1.03 ± 0.04
27 and 1.04 ± 0.04, in MCT2- and MCT4-KD rats, respectively, which confirms the absence of lactate
28 increase in these animals. No statistical difference was found between Ctrl (1.25 ± 0.05, n=23) and
29 uninjected rats (1.30 ± 0.09, n=16; p=0.0833).
30
31 To determine the origin of the lactate that accumulates during whisker activation, [1-^{13}C]glucose was
32 infused in awake rats. During the 1h-infusion, right whiskers were stimulated (same paradigm as the
33 one used for *in vivo* MRS, **Figure 2A**). At the end of the infusion, both right (at rest) and left (activated)
34 barrel cortices were removed (**Figure 2A**) and *ex vivo* MRS was performed on the perchloric acid
35 extracts using a proton-observed carbon-edited sequence. This sequence enabled the quantification of
36 some metabolite specific enrichments, which represent the percentage of ^{13}C incorporated into a carbon
37 position from the ^{13}C-labeled substrate that was infused (**Figure 2E**). For Ctrl rats, results indicate an
38 increase in the specific enrichment of lactate carbon 3 (C3) between rest (8.7%) and activated (11.3%)
39 barrel cortices (+30%), while the one of glutamine C4 decreased (from 11.1% to 7.3%). Since [3-^{13}C]
40 pyruvate, produced from [1-^{13}C]glucose at the end of the glycolysis, can either be converted into [3-
41 ^{13}C]lactate or go into the TCA cycle, from which [4-^{13}C]glutamine will be labeled (for a detailed fate of
42 [1-^{13}C]glucose, see (28)), the increase in [3-^{13}C]lactate specific enrichment together with a parallel
43 decrease in [3-^{13}C]glutamine specific enrichment in Ctrl rats during whisker stimulation reflects a relative
44 increase in glycolysis compared to the TCA cycle during activation, which was not observed in MCT-KD
45 rats. Indeed, for both MCT2- and MCT4-KD rats, no statistical difference between rest and activated
46 barrel cortices was found. Comparison of lactate C3 specific enrichments between the right barrel cortex
47 (resting hemisphere) and the left one (activated hemisphere) for each individual rat is shown in **Figure**
48 **2B** (Ctrl)**, C** (MCT2) and **D** (MCT4). For Ctrl rats, it can be clearly seen that whisker stimulation led to
49 an increase in the incorporation of ^{13}C in lactate, indicating that more [3-^{13}C]lactate was produced from
50 the infused precursor, [1-^{13}C]glucose, in the activated brain area. This was not observed for MCT2-KD
51 rats. Concerning MCT4-KD rats, two animals showed a clear increase in the specific enrichment of
52 lactate C3 between the right and the left hemispheres, whereas an obvious decrease was measured in
53 3 animals and slightly the same values were observed in 7 MCT4-KD rats.
54
55 *Cortical BOLD signal triggered by whisker activation requires MCT2-dependent neuronal lactate*
56 *shuttling provided at least in part by astrocytes via MCT4*
57
58 To understand why no metabolic response (observed as lactate accumulation) was detected in the
59 barrel cortex during whisker stimulation in MCT2- and MCT4-KD rats, BOLD fMRI was performed. The
60 5-min paradigm used during whisker stimulation was the same as the one used during *in vivo* MRS and

is presented **Figure 3A**. For Ctrl rats, a positive BOLD signal was recorded in 95% of the rats (**Figure 3B**, n=22). When the neuronal monocarboxylate transporter (MCT2) was downregulated, a positive BOLD fMRI signal was observed in only 12% of the animals. Moreover, in the 4 BOLD-positive MCT2-KD rats, brain activation level was much lower than in controls as shown in **Figure 3C** (only signals in BOLD responding animals were quantified). In the MCT4-KD group, 53% of the rats (9/17 animals; positively-responding rats) had a positive BOLD signal. For these MCT4-BOLD responding animals, no statistical difference was found in BOLD signal intensity compared to Ctrl rats. In contrast, 47% of the MCT4-KD rats (8/17 animals; non-responding rats) had no BOLD fMRI signals.

Rescue experiments were performed in Ctrl, MCT2-KD and MCT4-KD rats (**Figure 3E**). For those, a first BOLD fMRI was acquired, then lactate was infused *via* the tail vein to the animal, and a second BOLD fMRI was recorded,10min after starting lactate infusion (this time point was determined such as the lactate concentration in the barrel cortex, measured by *in vivo* MRS, was the highest with an increase of ~50%, **Figure 3D**). When sodium lactate was infused during whisker activation, no difference was observed in BOLD fMRI signals measured before or during lactate infusion, neither in Ctrl rats (similar positive BOLD fMRI signal before or during lactate infusion), nor in MCT2-KD rats (no BOLD signal, before or during lactate infusion). Interestingly, data for MCT4-KD animals can be clearly divided into two sub-groups; responding animals (during the first BOLD fMRI experiment, called MCT4 Resp) and non-responding animals (MCT4 Non resp). An increase in the BOLD fMRI signal was observed between the first (without lactate infusion) and the second (during lactate infusion) BOLD fMRI acquisitions in initially non-responding animals only (5/10 animals). Increases in signal between the first and the second BOLD fMRI acquisitions are shown in **Figure 3F**.

Learning involving the whisker-to-barrel system requires intact neuronal MCT2 expression and at least in part intact astroglial MCT4 expression in the barrel cortex

To determine if the absence of the BOLD signal in the barrel cortex upon whisker activation can lead to a loss of function, we developed a textured novel object recognition (tNOR) task to specifically probe a barrel cortex-dependent behavior. This task was designed to test the impact of MCT knockdowns in the barrel cortex on behavioral performance and was based on two already published protocols (29, 30). Some modifications were set up to avoid any texture recognition with the forepaws and to differentiate whisker-dependent sensory experience from whisker-independent experience (the protocol is presented in **Figure 4A** and objects are displayed in **Figure 4B**, left panel). As control, we used a classical visual novel object recognition task (vNOR; objects are presented in **Figure 4B**, right panel). The preference for one of the objects used was first evaluated and results indicated no preference for one of the objects for both vNOR and tNOR tasks (data not shown). The sensitivity and specificity of the test was also controlled using an N-methyl-D-aspartate (NMDA) injection in the barrel cortex to produce a localized excitotoxic lesion (31) and thus interfere with behavioral performance related to texture but not to visual information processing (**Figure 4C and D**). To analyze the impact of neuronal MCT2 downregulation in the barrel cortex, animals were submitted to the entire NOR protocol (**Figure 4E**). Unlike Ctrl rats, MCT2-KD animals were unable to discriminate between the two textures in the tNOR task, reflecting a dysfunction of the barrel cortex. Indeed, this impaired processing of somatosensory information prevented them to learn the task. However, in the vNOR task, their learning capacity was intact as they performed like Ctrl rats. Because of the striking visual difference between the two objects, an additional processing of somatosensory information (*via* whisking activity) was not necessary for recognition of the objects. Thus, the vNOR task can be considered to be barrel cortex-independent, most likely relying primarily on visual information processing. The impact of downregulating the astrocytic lactate transporter MCT4 was also explored using the NOR protocol (**Figure 4F**). Ctrl and MCT4-KD rats were both able to discriminate the objects during the vNOR task while Ctrl rats also succeeded in the tNOR task. In contrast, two distinct behaviors were observed for MCT4-KD rats in the tNOR task (**Figure 4G**). As already observed during BOLD fMRI experiments, MCT4-KD rats can be divided into two sub-groups; a first sub-group, that was clearly unable to discriminate the textured objects (discrimination index, 0.49 ± 0.04; 10/18 animals) while the second sub-group was able to discriminate the two different textured objects (discrimination index, 0.69 ± 0.06; 8/18 MCT4-KD rats).

Discussion
Three decades ago, a rise in lactate levels was observed for the first time in the visual cortex of humans by *in vivo* MRS during a photic stimulation (21, 22). At that time, this observation was attributed to a transient increase in glycolysis over respiration during brain activation. Recently, we developed a technique to perform similar *in vivo* MRS during brain activation in the rat barrel cortex (32). Using this

4

technique, our aim was to follow lactate fluctuations linked to brain activity (obtained by whisker stimulation) in animals in which key partners of the ANLS would be downregulated. Right whisker stimulation led to an increase in lactate content in the left barrel cortex (also called S1BF) in Ctrl rats (receiving the viral vector but expressing a non-specific sequence). The same increase in lactate was observed in non-injected rats, indicating that the stereotaxic injection of AAVs has no impact on our observed signal. Considering that brain lactate concentration was around 1 mM (measured in the barrel cortex at rest by *in vivo* MRS), this 25-30% increase would bring lactate concentration in the S1BF area around 1.25 - 1.30 mM. Keeping in mind the huge difference between neuronal activation and *in vivo* fMRS recording scales (ms *versus* min), this new lactate concentration may reflect a new steady state, in which the lactate concentration is enhanced, putatively to support high neuronal energy needs during brain activity. This new steady state in lactate concentration in the activated S1BF during whisker stimulation can be explained either by an increase in lactate synthesis during neuronal activity, or by a decrease in its consumption. To distinguish between these two hypotheses, we performed ^{13}C-experiments in which [1-^{13}C]glucose was infused in awake animals during right whisker activation. Then, both right and left barrel cortices were analyzed by *ex vivo* ^{1}H and ^{13}C-NMR spectroscopy. We measured an increase in the specific enrichment of [3-^{13}C] lactate in the activated S1BF in Ctrl rats. This means that neuronal stimulation led to a greater synthesis of lactate (^{13}C-labeled) in the activated zone, the precursor being [1-^{13}C]glucose infused in the blood circulation. This result confirms previous data obtained using *ex vivo* MRS on control rats (33), and indicate that lactate is produced from blood-circulating glucose within the brain area during neuronal activity, at least in the cortex.

When the neuronal lactate transporter MCT2 was downregulated in the rat barrel cortex, no lactate increase linked to whisker stimulation could be observed in this brain area. If we hypothesize that lactate is produced by astrocytes during brain activity, and is further transferred to neurons, it may be surprising not to observe an accumulation of lactate in these KD rats, in which lactate cannot enter neurons. To better understand this apparent paradox, we decided to perform BOLD fMRI experiments to detect signs of local brain activation (using the BOLD signal as a surrogate marker for activation). While a positive BOLD signal was observed in 95% of Ctrl rats, the BOLD signal was lost in MCT2 KD rats (only a small signal was observed in 4 out of 32 animals). These results confirm previous findings obtained using a lentiviral vector to express a similar shMCT2 sequence that prevented the BOLD response in the barrel cortex upon whisker stimulation (20). Based on these data, we can conclude that downregulation of the neuronal lactate transporter leads to the suppression of the mechanism which is at the origin of the BOLD signal, and therefore to an impairment of the neurovascular coupling. Since no increase in lactate levels was measured in fMRS experiments, MCT2 downregulation also leads to an apparent impairment of the neurometabolic coupling. Thus, it can be suggested that neuronal MCT2 downregulation alters somehow the mechanisms leading to neurovascular and neurometabolic responses occurring after a stimulation within the barrel cortex.

Similarly to MCT2, downregulation of the astroglial lactate transporter MCT4 in the rat barrel cortex prevented the lactate increase caused by whisker stimulation. In this regard, it seems that the neurometabolic coupling is impaired as well with astroglial MCT4 downregulation, emphasizing the importance of an intact lactate shuttling between astrocytes and neurons for this process. Surprisingly, for the BOLD signal, results obtained with MCT4 KD rats represent a dichotomous situation between those for Ctrl rats and the ones for MCT2 KD rats. Indeed, the BOLD signal was present in about half of the animals but absent in the other half, which suggests that local brain activation (and the associated neurovascular coupling) was not systematically lost (efficiency of MCT4 downregulation after stereotaxic injection in the S1BF was previously confirmed (27)). This situation suggests the existence of a threshold-like effect. Unlike neurons, which only have the MCT2 isoform, astrocytes express both isoforms 1 and 4. Moreover, they express lactate channels that also allow lactate release in an activity-dependent manner (34) and participate in lactate shuttling in awake mice (35). We can then assume that for MCT4 KD rats, the presence of MCT1 transporters as well as lactate channels still allows some lactate release. This export would be insufficient to measure by fMRS the same steady state level as the one measured in Ctrl rats upon activation, but would be sufficient, at least in some rats, to maintain the appearance of the BOLD signal in the activated zone. Indeed, if enough lactate comes out of astrocytes, or is sufficiently present in the extracellular space, it can then be sensed by neurons (MCT2 is still present). If used extensively, such as during brain activation, then lactate cannot accumulate in the extracellular space and no increase can be measured during *in vivo* fMRS. According to this hypothesis, astrocytes would therefore supply under physiological conditions more lactate than is necessary for neurons, which is in accordance with the new steady state level of lactate concentration that is measured. We may hypothesize that a lactate concentration threshold may exist to support brain

activation, which was reached only in half of the MCT4 KD rats. This hypothesis would also fit with rescue experiments, in which lactate infusion was able to rescue the BOLD signal in non-responding MCT4 animals.

Altogether, our data suggest that lactate supply to neurons by astrocytes could somehow regulate neuronal network activity and define a new threshold of excitability. This effect would be entirely prevented by neuronal MCT2 downregulation but not systematically following astroglial MCT4 downregulation, depending on the resulting lactate levels which may fluctuate (according to the extent of astroglial MCT4 downregulation). Indeed, several evidence have been provided that lactate can act as a signal to modulate neuronal excitability (10). This action of lactate could be mediated via several described mechanisms, including an effect on NMDA receptors, on pH, on ATP-sensitive potassium channels or on lactate receptors. It is purported that such an effect of lactate over a region corresponding to a barrel within the S1BF area would promote the capacity of the neuronal network within that structure to fine tune in a coordinated manner neuronal processing and promote learning and memory processes.

The possibility that reducing neuronal MCT2 expression or astroglial MCT4 expression might also interfere with behavioral performance that relies on the activation of the barrel cortex was tested. MCT2 downregulation led to an important deficit of S1BF function, reflected by the absence of discrimination between the objects during the tNOR task. However, those animals were still able to discriminate the objects during the vNOR task. Results obtained in astroglial MCT4 downregulated animals reflected those obtained in BOLD fMRI experiments. About half of the animals were impaired in the tNOR task. These results show that the memory deficit seen in the tNOR task was caused by a specific deficit in the processing of somatosensory information in the barrel cortex, and not a global impairment in learning or a deficit related to the other brain structures involved in the task. These findings concur with several others indicating that interfering with MCT expression on astrocytes and neurons, and/or lactate shuttling between the two cell types, alters learning and memory performances in a number of spatial and non-spatial tasks (36-41). While previous studies were targeting either the hippocampus or the striatum, our study is demonstrating an effect on behavioral performance after modifying expression in a specific cortical area. This finding reinforces the view that lactate shuttling between astrocytes and neurons is a fundamental process present in various brain regions that is essential to sustain cognition.

In conclusion, our data indicate that lactate shuttling *via* MCTs between astrocytes and neurons is necessary to give rise to both neurovascular and neurometabolic couplings linked to brain activity. Since functional brain imaging relies on signals arising from these processes to map brain activity, our findings emphasize the key contribution of astrocytes to brain imaging. Finally, as lactate shuttling was found here to be a limiting factor to sustain cognitive function subserved by local cortical activation, it becomes of interest to consider the role of this astrocyte-dependent mechanism in the context of neurodegenerative diseases. Indeed, as cortical hypometabolism is a classical observation in these pathologies and has been evidenced even at asymptomatic stages, astrocytes and their regulation of energy metabolism might constitute a novel preventive therapeutic target.

Materials and Methods
Data and associated protocols that support the findings of this study are available upon request from the corresponding author.
1. Animals
All animal procedures were conducted in accordance with the Animal Experimentation Guidelines of the European Communities Council Directive of November 24, 1986 (86/609/EEC). Protocols met the ethical guidelines of the French Ministry of Agriculture and Forests, and were approved by the local ethics committees (Comité d'éthique pour l'expérimentation Animale Bordeaux n°50112090-A and the Swiss "Service de la Consommation et des Affaires Vétérinaires, SCAV, authorization n°3101.1). Male Wistar RJ-HAN (Janvier Laboratories, France) were kept on a 12:12 hours light:dark cycle with food and water *ad libitum*.
2. AAV2/DJ-based viral vector generation
AAV2/DJ-based viral vectors were prepared exactly as described in detail in Jollé *et al.* (45). Briefly, four constructs were made to target alternatively neurons or astrocytes. For neuron-specific expression, a shRNA sequence targeting MCT2 (shMCT2; TAGGATTAATAGCCAACACTA) or a control non-coding sequence (shUNIV2; TGTATCGATCACGAGACTAGC) embedded in a miR30E sequence was positioned after a mCherry sequence under the control of a CBA (Chicken-β-actin) promoter. For astrocyte-specific expression, a shRNA sequence targeting MCT4 (shMCT4;

GGTGAGCTATGCTAAGGATAT) or a control non-coding sequence (shUNIV4; TGTATCGATCACGAGACTAGC) embedded in a miR30E sequence was positioned after a mCherry sequence under the control of a G1B3 (a Glial Fibrillary Acidic Protein derived) promoter (42). Each construct was incorporated in an AAV2/DJ serotype to obtain four distinct AVV2/DJ-based viral vectors. All these viral vectors had been tested previously for their specificity and efficacy in the rat barrel cortex (45). Since no difference was observed between animals injected with either AAV2/DJ-CBA-shUNIV2 or AAV2/DJ-G1B3-shUNIV4, data from these animals were pooled and considered as control (Ctrl) data.

3. Stereotaxic injection

Surgeries were performed on seven-week-old animals. Animals were anesthetized with isoflurane (5% for the induction and 3% to maintain the anesthesia). AAVs or PBS were injected in one site/hemisphere (S1BF: Anteroposterior = - 2,3 mm; Mediolateral = ± 5 mm; Dorsoventral = - 3 mm). Viral vectors were injected with 34G steel cannula fixed on a cannula holder and linked to a 10 μL Hamilton syringe and an infusion pump. For each site, 4 μL of viral vector were injected at 0.2 μL/min. Cannulas were left in the brain for 5 minutes after the injection, and then slowly removed. Skin was closed using 4.0 sterile suture thread. Sterile NaCl 0.9% solution (1 mL) was delivered to the rat by intra-peritoneal injection to avoid dehydration after surgery, and healing cream was applied on the head. Sugar-taste Paracetamol was delivered to the animal in water (1g/cage for rats) during 72h. Animals were monitored until complete awakening, and every day during three days after the surgery. All viral vectors were injected at a final concentration of $1x10^8$ vg/site.

4. *In vivo* functional ^{1}H-MRS and BOLD fMRI

Experiments were conducted on a 7T Bruker BioSpec system (70/20, Ettlingen, Germany) equipped with a 20-cm horizontal bore, a gradient system capable of 660 mT/m maximum strength and 110μs rise time. A surface coil (10-mm inner diameter, Bruker) was used for excitation and signal reception. Rats were anaesthetized using medetomidine hydrochloride (Domitor, Vetoquinol SA, France, 1 mg/mL, 240 μg/kg/h – perfusion rate: 20 μL/min). Whisker activation was performed directly into the magnet using an air-puff system (32). For this purpose, right whiskers were taped such as a sail was made and this sail was blown at 8 Hz during the acquisition time (activation paradigm: 20s activation – 10s rest, duration 5min20s for fMRS and 5min for fMRI). In order to place correctly the voxel in the S1BF area, a T$_2$-weighted sequence was performed (RARE sequence): 16 slices, 1 mm thick, FOV 5x5 cm. A voxel was then located in the S1BF area (2 x 2.5 x 3 mm) and *in vivo* spectroscopy was performed either at rest or during whisker activation using a LASER sequence (TE 20 ms, TR 2500 ms, 128 scans). Spectra were analyzed and lactate was quantified using LCModel (Provencher) software using water-scaling (WCONC 43300).

Finally, functional imaging was performed. The BOLD response was measured (using the activation paradigm) in four slices of 0.7 mm thickness using a single short gradient echo, echo planar imaging sequence (TR = 500ms, TE = 16.096ms, field of view 25x25 mm², matrix size 96x96 and bandwidth of 33333 Hz). Images were reconstructed and analyzed using FUN TOOL fMRI processing (Bruker software).

5. Rescue experiments

Rats were anaesthetized using medetomidine hydrochloride (Domitor, Vetoquinol SA, France, 1 mg/mL, 240 μg/kg/h – perfusion rate: 20 μL/min) as previously, using an amagnetic tail vein catheter. A three-way stopcock was used for lactate infusion (sodium salt, 534 mM, with a flow rate monitored from 15 mL/h to 1.23 mL/h during the first 25min (1)). Measurement of the BOLD response was performed twice. The first acquisition was performed during whisker activation, without lactate infusion. Then, lactate infusion was initiated and, 10min later, the second BOLD experiment was started. Lactate concentration was the highest in the barrel cortex in this time window, as previously determined by *in vivo* ^{1}H-MRS performed every 5min in the barrel cortex during the lactate infusion protocol period (25min).

6. *Ex vivo* MRS

Whisker activation on awake animals. Experiments were performed in awake animals six weeks after AAV injection. Animals were slightly held on a Plexiglas support during the stimulation. Before infusion experiments, each animal was accustomed to the experimental set up (at least 3 times, 1h) to avoid any stress and ^{13}C-infusion experiments were performed once rats demonstrated that they lie quietly. Right whiskers were mechanically stimulated at a rate of 8 Hz during 1h. To stimulate the maximum of whiskers, they were cut to an equivalent length: 2.5 cm. Infusions were performed in the tail vein during 1h (to reach the isotopic steady state), during the whisker stimulation. Rats were infused with a solution containing [1-^{13}C glucose] (750 mM, Cambridge isotope, 99% enrichment) + lactate (sodium salt, 534 mM). Intravenous infusions were carried out using a syringe pump that allows a flux such as glucose and lactate concentrations in the blood remain constant (the infusate flow was monitored to obtain a time-decreasing exponential from 15 mL/h to 1.23 mL/h during the first 25min after which the rate was kept unchanged). At the end of the experiment, a sample of blood was removed; rats were rapidly

1 euthanized by cerebral-focused microwaves (5 KW, 1s, Sacron8000, Sairem), the only way to
2 immediately stop all enzymatic activities and to avoid post-mortem artefacts such as anaerobic lactate
3 production, as already demonstrated in (33).
4 S1BF areas (right -non activated- and left -activated-) were removed, using a rat brain matrix that allows
5 precise and reproducible dissection of the selected brain regions, dipped in liquid nitrogen and kept at -
6 80°C until NMR analyses, conducted on a Bruker DPX500 spectrometer equipped with a HRMAS (High
7 Resolution at the Magic Angle Spinning) probe after perchloric acid extracts. Indeed, HR-MAS allows
8 performing spectra with high spectral resolution not only directly on biopsies but also on small perchloric
9 acid extract volumes (50 μL).
10 *Perchloric acid extracts*: A volume of 200 μL of 0.9 M perchloric acid was added to the frozen S1BF
11 biopsies (around 30 mg) and further sonicated (at 4°C). The mixture was then centrifuged at 5000 g for
12 15min (4°C). The brain extract was neutralized with KOH to pH=7.2, centrifuged again to eliminate
13 potassium perchlorate salts. Supernatant was lyophilized, the final powder was dissolved in 100 μL D_2O
14 and bivalent cations were eliminated using Chelex^{TM} 100 resin beads. Ethylene glycol was added and
15 used as an external reference (1 M, peak at 63 ppm, 2 μl).
16 *Proton-observed carbon-editing (POCE) sequence*: This sequence was used to determine the ^{13}C-
17 specific enrichment (SE) at selected metabolite carbon positions using the (^{13}C-^{1}H) heteronuclear
18 multiquanta correlation (43, 44). Briefly, two spectra are acquired: the first scan corresponds to a
19 standard spin-echo experiment without any ^{13}C excitation and a second scan involves a ^{13}C-inversion
20 pulse to get coherence transfer between coupled ^{13}C and ^{1}H nuclei. Subtraction of two alternate scans
21 leads to the editing of ^{1}H spins coupled to ^{13}C spins (scalar coupling constant JCH = 127 Hz). ^{13}C-
22 decoupling was applied during the acquisition to collapse the ^{1}H-^{13}C coupling under a single 1H
23 resonance. Flip angles for rectangular pulses were carefully calibrated on both radiofrequency channels
24 before each experiment. The relaxation delay was 8s for a complete longitudinal relaxation. The ^{13}C-SE
25 was calculated as the ratio of the area of a given resonance on the edited ^{13}C-^{1}H spectrum to its area
26 on the standard spin-echo spectrum. The reproducibility and accuracy of the method were previously
27 assessed using several mixtures of ^{13}C-labeled amino acids and lactate with known fractional
28 enrichments and both were better than 5%.
29 **7. Behavioral studies**
30 Animals were given three weeks to recover from surgery (AAV injections). They were habituated to the
31 housing of the behavioral area for two weeks. During the first two days of behavioral testing, rats were
32 habituated for 10min to the circular open field arena (45 x 10 cm, light grey). The floor and walls were
33 cleaned with ethanol 70% to avoid scent trails guiding the animals between test sessions. On the third
34 day, the textured task of the NOR (tNOR) was performed. For the first step, the animal was released on
35 one side of the arena, facing the wall, at equal distance from the two identical objects. The objects were
36 placed equidistant from the center of the arena and from the walls. Each rat was allowed to explore the
37 objects for 10min. The animal was then removed from the arena for 5min. During this retention period,
38 the arena and the objects were wiped with ethanol 70%. One of the familiar objects was replaced by the
39 novel object. This object was visually identical to the familiar object (in size, shape, colour) but exhibited
40 a different texture (smooth or rough). To avoid any texture discrimination coming from forepaws and to
41 test only whisker sensitivity, only the lower part of the object had a different texture. Then for the second
42 step, the rat was returned into the test arena and allowed to explore the objects for 10min. The time
43 each rat spent physically exploring the objects was recorded during both steps.
44 On the fourth day, the visual task of the NOR (vNOR) took place. The rat was allowed to explore the
45 two identical objects for 10min. Then the rat was removed from the arena for 5min. The arena and
46 objects were wiped with ethanol 70%. One object was replaced by a novel object. This object was
47 visually different from the familiar one. Then the animal was reintroduced into the arena and allowed to
48 explore the objects for 10min.
49 In the visual task, object A was 10 cm in diameter x 22 cm in height and object B was 10 x 10 x 20 cm.
50 In the textured task, the two objects were 10.5 x 5 x 15.5 cm. Object A was rough and Object B was
51 smooth.
52 The novelty preference index was calculated as $Preference\ Index = \frac{Time_{Object\ A/B}}{(Time_{Object\ A} + Time_{Object\ B})}$. Animals
53 that did not explore the two objects for at least 4 seconds were excluded from the analysis. The visual
54 (vNOR) and the textured (tNOR) tasks were recorded using Media Recorder v.4.0.2. The time of
55 exploration was blindly and manually scored using Kinoscope v0.3.0.
56
57 **8. Statistical analysis**
58 Results are presented as mean ± SEM. Statistical analyses were performed with GraphPad Prism (v.
59 7.04). For behavioral analyses, a Wilcoxon's test was applied to compare the novelty preference index

to 0.5 (chance value). For BOLD fMRI and fMRS, data were analyzed using ordinary one-way ANOVA followed by a Fisher's LSD test or paired-t test. Results were considered significant when $p < 0.05$.

Acknowledgments

References

1.   A. K. Bouzier *et al.*, The metabolism of [3-(13)C]lactate in the rat brain is specific of a pyruvate carboxylase-deprived compartment. *J Neurochem* **75**, 480-486 (2000).

2.   D. Smith *et al.*, Lactate: a preferred fuel for human brain metabolism in vivo. *J Cereb Blood Flow Metab* **23**, 658-664 (2003).

3.   G. van Hall *et al.*, Blood lactate is an important energy source for the human brain. *J Cereb Blood Flow Metab* **29**, 1121-1129 (2009).

4.   F. Boumezbeur *et al.*, The contribution of blood lactate to brain energy metabolism in humans measured by dynamic 13C nuclear magnetic resonance spectroscopy. *J Neurosci* **30**, 13983-13991 (2010).

5.   L. Pellerin, P. J. Magistretti, Glutamate uptake into astrocytes stimulates aerobic glycolysis: a mechanism coupling neuronal activity to glucose utilization. *Proc Natl Acad Sci U S A* **91**, 10625-10629 (1994).

6.   A. K. Bouzier-Sore *et al.*, Competition between glucose and lactate as oxidative energy substrates in both neurons and astrocytes: a comparative NMR study. *Eur J Neurosci* **24**, 1687-1694 (2006).

7.   A. K. Bouzier-Sore, P. Voisin, P. Canioni, P. J. Magistretti, L. Pellerin, Lactate is a preferential oxidative energy substrate over glucose for neurons in culture. *J Cereb Blood Flow Metab* **23**, 1298-1306 (2003).

8.   L. Pellerin, P. J. Magistretti, Sweet sixteen for ANLS. *J Cereb Blood Flow Metab* **32**, 1152-1166 (2012).

9.   L. F. Barros, B. Weber, CrossTalk proposal: an important astrocyte-to-neuron lactate shuttle couples neuronal activity to glucose utilisation in the brain. *J Physiol* **596**, 347-350 (2018).

10.   P. J. Magistretti, I. Allaman, Lactate in the brain: from metabolic end-product to signalling molecule. *Nat Rev Neurosci* **19**, 235-249 (2018).

11.   G. Bonvento, J. P. Bolanos, Astrocyte-neuron metabolic cooperation shapes brain activity. *Cell Metab* **33**, 1546-1564 (2021).

12.   A. Volkenhoff *et al.*, Glial Glycolysis Is Essential for Neuronal Survival in Drosophila. *Cell Metab* **22**, 437-447 (2015).

13.   L. Liu, K. R. MacKenzie, N. Putluri, M. Maletic-Savatic, H. J. Bellen, The Glia-Neuron Lactate Shuttle and Elevated ROS Promote Lipid Synthesis in Neurons and Lipid Droplet Accumulation in Glia via APOE/D. *Cell Metab* **26**, 719-737 e716 (2017).

14.   F. Baeza-Lehnert *et al.*, Non-Canonical Control of Neuronal Energy Status by the Na(+) Pump. *Cell Metab* **29**, 668-680 e664 (2019).

15.   C. M. Diaz-Garcia *et al.*, Neuronal Stimulation Triggers Neuronal Glycolysis and Not Lactate Uptake. *Cell Metab* **26**, 361-374 e364 (2017).

16.   J. J. Laschet *et al.*, Glyceraldehyde-3-phosphate dehydrogenase is a GABA$_A$ receptor kinase linking glycolysis to neuronal inhibition. *J Neurosci* **24**, 7614-7622 (2004).

17.   A. Herrero-Mendez *et al.*, The bioenergetic and antioxidant status of neurons is controlled by continuous degradation of a key glycolytic enzyme by APC/C-Cdh1. *Nature cell biology* **11**, 747-752 (2009).

18.   L. K. Fellows, M. G. Boutelle, M. Fillenz, Physiological stimulation increases nonoxidative glucose metabolism in the brain of the freely moving rat. *J Neurochem* **60**, 1258-1263. (1993).

19.   Y. Hu, G. S. Wilson, A temporary local energy pool coupled to neuronal activity: fluctuations of extracellular lactate levels in rat brain monitored with rapid-response enzyme-based sensor. *J Neurochem* **69**, 1484-1490. (1997).

20. L. Mazuel *et al.*, A neuronal MCT2 knockdown in the rat somatosensory cortex reduces both the NMR lactate signal and the BOLD response during whisker stimulation. *PLoS One* **12**, e0174990 (2017).

21. J. Prichard *et al.*, Lactate rise detected by 1H NMR in human visual cortex during physiologic stimulation. *Proc Natl Acad Sci U S A* **88**, 5829-5831 (1991).

22. D. Sappey-Marinier *et al.*, Effect of photic stimulation on human visual cortex lactate and phosphates using 1H and 31P magnetic resonance spectroscopy. *J Cereb Blood Flow Metab* **12**, 584-592 (1992).

23. K. Pierre, L. Pellerin, Monocarboxylate transporters in the central nervous system: distribution, regulation and function. *J Neurochem* **94**, 1-14 (2005).

24. K. Pierre, P. J. Magistretti, L. Pellerin, MCT2 is a major neuronal monocarboxylate transporter in the adult mouse brain. *J Cereb Blood Flow Metab* **22**, 586-595 (2002).

25. K. Rosafio, X. Castillo, L. Hirt, L. Pellerin, Cell-specific modulation of monocarboxylate transporter expression contributes to the metabolic reprograming taking place following cerebral ischemia. *Neuroscience* **317**, 108-120 (2016).

26. O. Chiry *et al.*, Expression of the monocarboxylate transporter MCT1 in the adult human brain cortex. *Brain Res* **1070**, 65-70 (2006).

27. C. Jolle, N. Deglon, C. Pythoud, A. K. Bouzier-Sore, L. Pellerin, Development of Efficient AAV2/DJ-Based Viral Vectors to Selectively Downregulate the Expression of Neuronal or Astrocytic Target Proteins in the Rat Central Nervous System. *Front Mol Neurosci* **12**, 201 (2019).

28. A. K. Bouzier, B. Quesson, H. Valeins, P. Canioni, M. Merle, [1-(13)C]glucose metabolism in the tumoral and nontumoral cerebral tissue of a glioma-bearing rat. *J Neurochem* **72**, 2445-2455 (1999).

29. V. Briz *et al.*, The non-coding RNA BC1 regulates experience-dependent structural plasticity and learning. *Nature communications* **8**, 293 (2017).

30. H. P. Wu, J. C. Ioffe, M. M. Iverson, J. M. Boon, R. H. Dyck, Novel, whisker-dependent texture discrimination task for mice. *Behavioural brain research* **237**, 238-242 (2013).

31. E. D. Kirby, K. Jensen, K. A. Goosens, D. Kaufer, Stereotaxic surgery for excitotoxic lesion of specific brain areas in the adult rat. *J Vis Exp* 10.3791/4079, e4079 (2012).

32. J. Blanc *et al.*, Functional Magnetic Resonance Spectroscopy at 7 T in the Rat Barrel Cortex During Whisker Activation. *J Vis Exp* 10.3791/58912 (2019).

33. D. Sampol *et al.*, Glucose and lactate metabolism in the awake and stimulated rat: a (13)C-NMR study. *Front Neuroenergetics* **5**, 5 (2013).

34. T. Sotelo-Hitschfeld *et al.*, Channel-mediated lactate release by K(+)-stimulated astrocytes. *J Neurosci* **35**, 4168-4178 (2015).

35. M. Zuend *et al.*, Arousal-induced cortical activity triggers lactate release from astrocytes. *Nat Metab* **2**, 179-191 (2020).

36. G. Descalzi, V. Gao, M. Q. Steinman, A. Suzuki, C. M. Alberini, Lactate from astrocytes fuels learning-induced mRNA translation in excitatory and inhibitory neurons. *Commun Biol* **2**, 247 (2019).

37. D. L. Korol, R. S. Gardner, T. Tunur, P. E. Gold, Involvement of lactate transport in two object recognition tasks that require either the hippocampus or striatum. *Behav Neurosci* **133**, 176-187 (2019).

38. C. Netzahualcoyotzi, L. Pellerin, Neuronal and astroglial monocarboxylate transporters play key but distinct roles in hippocampus-dependent learning and memory formation. *Prog Neurobiol* **194**, 101888 (2020).

39. M. Tadi, I. Allaman, S. Lengacher, G. Grenningloh, P. J. Magistretti, Learning-Induced Gene Expression in the Hippocampus Reveals a Role of Neuron-Astrocyte Metabolic Coupling in Long Term Memory. *PLoS One* **10**, e0141568 (2015).

40. L. A. Newman, D. L. Korol, P. E. Gold, Lactate produced by glycogenolysis in astrocytes regulates memory processing. *PLoS One* **6**, e28427 (2011).

41. A. Suzuki *et al.*, Astrocyte-neuron lactate transport is required for long-term memory formation. *Cell* **144**, 810-823 (2011).

42. M. Humbel *et al.*, Maximizing lentiviral vector gene transfer in the CNS. *Gene Ther* **28**, 75-88 (2021).

43. R. Freeman, T. H. Mareci, G. A. Morris, Weak satellite signals in high-resolution NMR spectra: separating the wheat from the chaff. *J Magn Reson* **42**, 341-345 (1981).

44. D. L. Rothman *et al.*, 1H-Observe/13C-decouple spectroscopic measurements of lactate and glutamate in the rat brain in vivo. *Proc Natl Acad Sci U S A* **82**, 1633-1637. (1985).
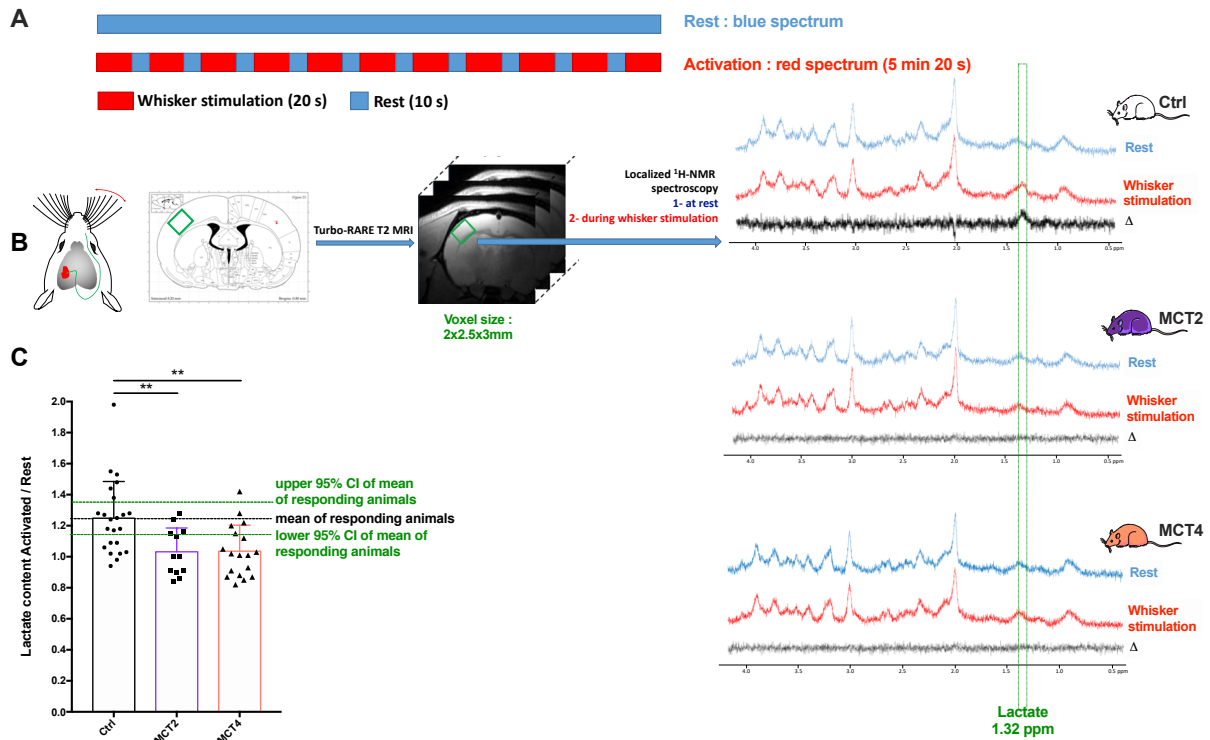
Figures
2
3

4
5   **Figure 1.** *In vivo* **functional MRS upon whisker stimulation in rats with cell-specific MCT2 or MCT4**
6   **downregulation in the barrel cortex. A:** Whisker stimulation paradigm (activation: 20s, 8Hz; rest: 10s
7   to avoid neuronal desensitization, during the entire MRS acquisition for the activation condition: 128
8   scans, 5min20s). **B:** The right whisker stimulation leads to the activation of the barrel cortex (also called
9   S1BF) in the left somatosensory cortex. Voxel location for MRS is determined by comparison of T2-
10 weighted images and rat atlas maps. Typical spectra acquired at rest (blue) and during whisker
11 stimulation (red) for Ctrl, MCT2- and MCT4-KD rats. The difference between the red and the blue spectra
12 is shown in the black spectra. The green rectangle indicates the chemical shift of the protons from the
13 methyl group of lactate (protons linked to lactate carbon 3) at 1.32ppm. **C:** Ratio of lactate contents
14 during the whisker stimulation and the resting state. Ctrl, n=23; MCT2, n=12; MCT4, n=18. ** $p<0.004$,
15 one-way ANOVA followed by a Fisher's LSD test.
16

1
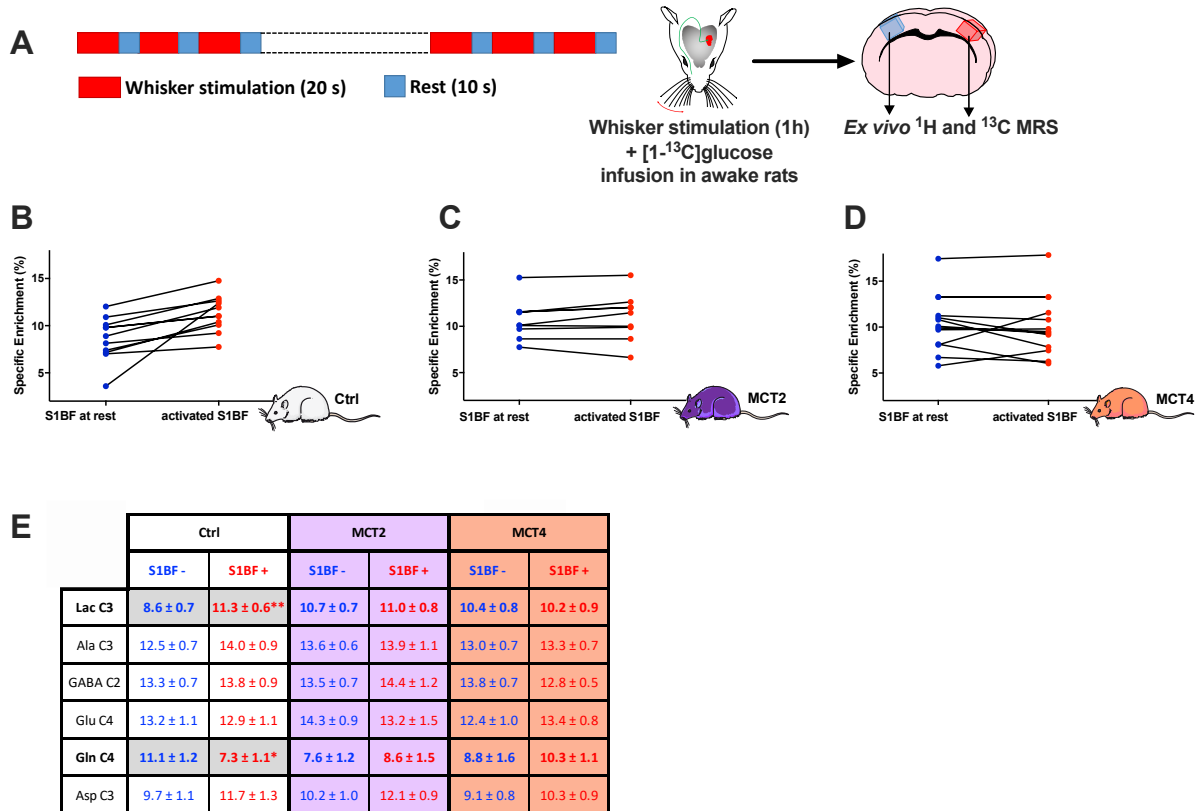
Figure 2. **Comparison of lactate C3 ^{13}C-specific enrichments (%) between the resting hemisphere (right S1BF, blue) and the activated hemisphere (left S1BF, red). A:** Paradigm used for whisker stimulation (activation: 20s, 8Hz; rest: 10s, during the entire [1-^{13}C]glucose infusion protocol: 1h). **B:** Comparison of [3-^{13}C]lactate specific enrichment (%) for each animal between the resting and activated S1BF in Ctrl rats, n=11, ** p=0.004, between right and left hemispheres, paired t-test. **C:** Comparison of [3-^{13}C]lactate specific enrichment (%) for each animal between the resting and activated S1BF in MCT2 rats, n=9. **D:** Comparison of [3-^{13}C]lactate specific enrichment (%) for each animal between the resting and activated S1BF in Ctrl rats, n=13. **E:** Means values of [3-^{13}C]lactate specific enrichment (%), in the resting (Ctrl-, MCT2- and MCT4-) and in the activated (Ctrl+, MCT2+ and MCT4+) hemispheres, ** p=0.004, between right and left hemispheres, paired t-test. **F:** ^{13}C-specific enrichment values for some metabolites (%). [1-^{13}C]glucose was infused in the tail vein and the ^{13}C incorporation in some metabolites was measured from POCE spectra of perchloric acid extracts of resting and activated S1BF in Ctrl, MCT2 and MCT4 rats. Lac C3: carbon 3 of lactate; Ala C3: carbon 3 of alanine; GABA C2: carbon 2 of γ−aminobutyrate; Glu C4: carbon 4 of glutamate; Gln C4: carbon 4 of glutamine and Asp C3: carbon 3 of aspartate. * p<0.05, ordinary one-way ANOVA, followed by Fisher's LSD test. Ctrl, n=11; MCT2, n=9 and MCT4, n=13.
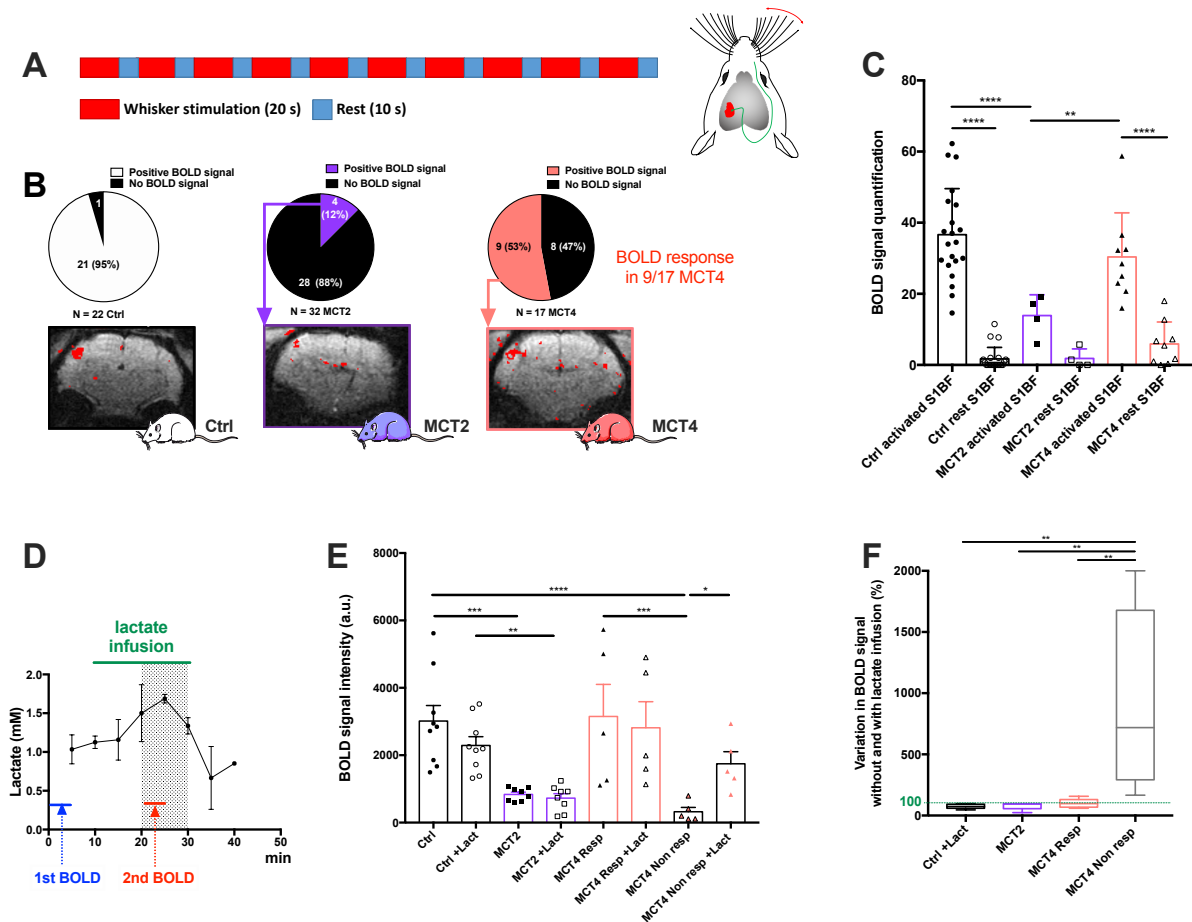
1
2 **Figure 3. Effect of cell-specific MCT2 or MCT4 downregulation in the barrel cortex on the BOLD**
3 **fMRI response during whisker stimulation and its putative rescue by lactate infusion. A:** Whisker
4 stimulation paradigm (activation: 20s, 8Hz; rest: 10s, during the entire fMRI acquisition: 600 scans,
5 5min). **B:** Distribution of positively/negatively responding animals and typical BOLD fMRI images for Ctrl
6 (n=22), MCT2-KD (n=32) and MCT4-KD (n=17) rats. **C:** Quantification of BOLD fMRI signals (only for
7 positively-responding animals). **D:** Lactate concentration kinetics in the barrel cortex during peripheral
8 lactate infusion. Lactate content was determined every 5min by localized ^{1}H-NMR spectroscopy in the
9 barrel cortex during lactate infusion (20min) in the tail vein. The highest lactate concentration is reached
10 in the shaded grey zone. Based on this kinetics, the best time window to acquire the second BOLD fMRI
11 was selected (red line). n=2. **E:** Rescue experiments: BOLD fMRI was performed before (closed
12 symbols) and 10min after starting lactate infusion (open symbols) in Ctrl (n= 9, circles), MCT2-KD (n=8,
13 squares) and MCT4-KD (n=10, triangles) rats. * $p<0.05$; ** $p<0.01$; *** $p<0.001$; **** $p<0.0001$; ANOVA
14 followed by a Fisher's LSD test. **F:** Variation in BOLD signal intensity between acquisitions (shown in **E**)
15 performed before and during lactate infusion (%, minimum to maximum and median). ** $p<0.01$; ANOVA
16 followed by a Fisher's LSD test. The dashed green line represents no variation (100%).
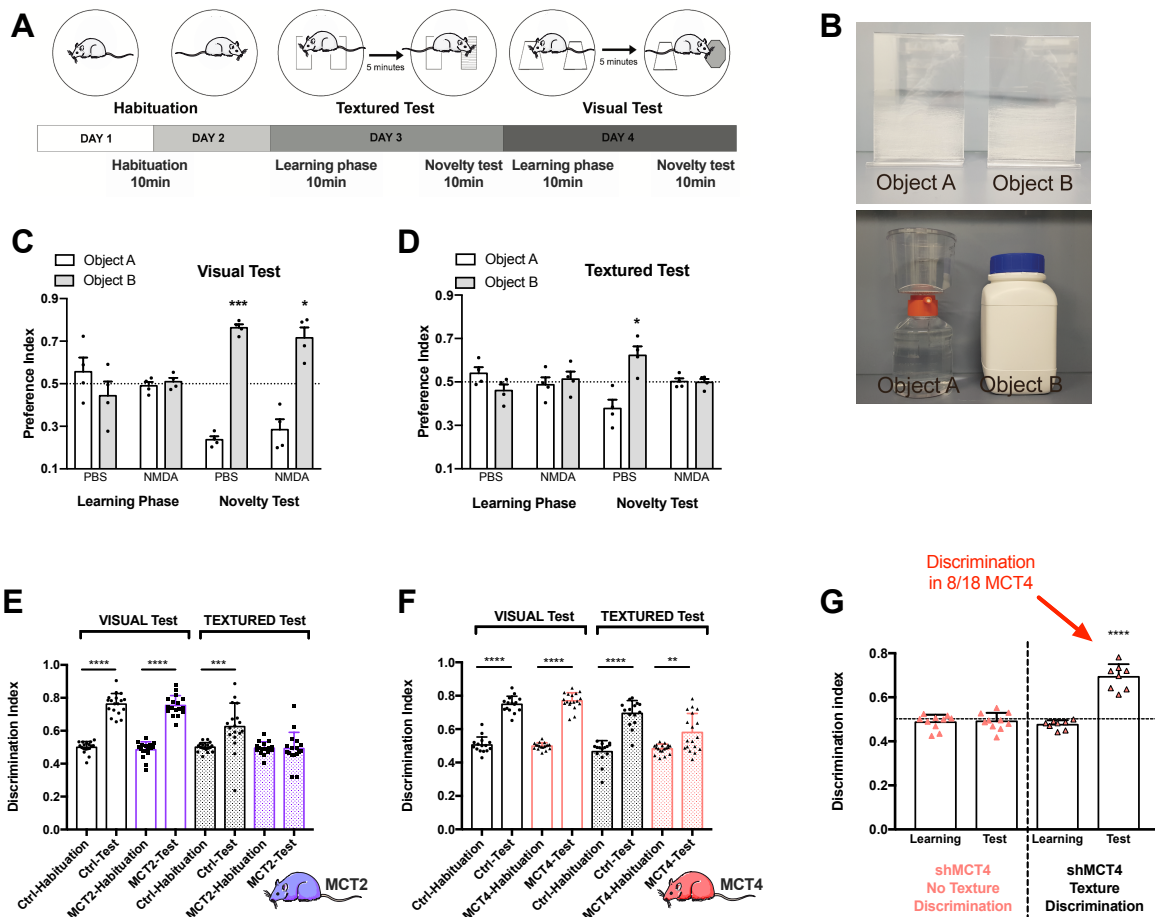
1
2 **Figure 4. Effect of cell-specific MCT2 or MCT4 downregulation in the barrel cortex on**
3 **performance in the visual and textured novel object recognition tasks**

4 **A:** Schematic representation of the protocol to perform both the textured and visual novel recognition
5 tasks. The test is divided in 4 consecutive days. On day 1 and 2, animals were habituated to the arena
6 for 10min. On the third day, the animal was submitted to the textured task, composed of 10min of
7 learning, 5min of rest and 10min of test with one of the objects that was exchanged. In the textured task,
8 the novel object was identical in size, shape and color but different in term of texture (smooth versus
9 rough). Finally, on the fourth day, the animal was submitted to the visual task and for the visual task.
10 The difference with the third day was that the novel object was different in term of shape and color. For
11 the two last days, the time spent exploring the objects was measured. **B:** Pictures of the objects used
12 for the textured and visual tasks. **C:** Effect of an excitotoxic lesion in the barrel cortex on performance
13 in the visual novel object recognition tasks; preference indexes for the visual task of animals injected
14 with PBS (Phosphate buffered saline) or NMDA (N-methyl D-aspartate) 1M. The dashed line
15 corresponds to chance level, when the animal equally explored the two objects. Data are presented as
16 mean ± SEM. * $p<0.05$, *** $p<0.001$, ordinary one-way ANOVA, followed by Fisher's LSD test. n=6 rats.
17 **D:** Effect of an excitotoxic lesion in the barrel cortex on performance in the textured novel object
18 recognition tasks; preference indexes for the textured task of animals injected with PBS or NMDA 1M.
19 The dashed line corresponds to chance level, when the animal equally explored the two objects. Data
20 are presented as mean ± SEM. * $p<0.05$, ordinary one-way ANOVA, followed by Fisher's LSD test. n=6.
21 **E:** Discrimination indexes for the visual and the textured NOR for Ctrl and MCT2 animals. Data are
22 presented as mean ± SEM. *** $p<0.001$; **** $p<0.0001$, unpaired t-test between habituation and test.
23 Ctrl, n=18; MCT2, n=16. **F:** Discrimination indexes for the visual and the textured NOR for Ctrl and
24 MCT4 animals. Data are presented as mean ± SEM. ** $p<0.01$; **** $p<0.0001$, unpaired t-test between
25 habituation and test. Ctrl, n=15; MCT4, n=18. **G:** Discrimination indexes for the learning and the test
26 phases of the tNOR task for MCT4 animals, which was divided in two groups (n=18). Orange triangles:
27 MCT4 animals with no texture discrimination, n=10; black and orange triangles: MCT4 animals with
28 texture discrimination, n=8. Data are presented as mean ± SEM. **** $p<0.0001$. The horizontal black
29 dashed line corresponds to an equal exploration of the two objects.